J. Fluid Mech. (1968), *vol.* 33, *part* 1, *pp.* 131–149
Printed in Great Britain

An analytical and experimental investigation of the velocities of particles entrained by the gas flow in nozzles

By JOHN H. NEILSON AND ALASTAIR GILCHRIST
The University of Strathclyde, Glasgow

(Received 13 September 1967)

Among the parameters which determine the erosion damage sustained by the walls of a nozzle, in which a mixture of gas and particles is flowing is the speed attained by the particle before collision with the wall surface. This work is concerned with the determination of the particle velocity, and a number of relationships are given from which the variation in particle velocity can be obtained for a variety of gas conditions. The changes of state and velocity of the gas, occasioned by the interchange of heat and work between the gas and the particles are dependent on the ratio of the mass flow rate of particles to the mass flow rate of gas. It is shown that if this ratio is small the particle velocity may be obtained without serious error by assuming that the gas conditions are not affected by the presence of particles. Figures for the limiting value of this ratio for certain flows are given. The effects of particle size, density and initial relative velocity are investigated analytically and experimentally.

1. Introduction

This investigation was part of a study of the erosion damage sustained by nozzles passing a mixture of gas and particles, with particular reference to that part of the erosion in rocket motor tail nozzles which can be attributed to the action of particles produced in the combustion chamber. The erosion suffered by the nozzle wall at a given cross-section in the flow was shown to depend on the properties of the wall material, the total mass of impinging particles, the particle speed and the angle of attack. Thus it was necessary to investigate the factors which determine the way in which the particle velocity varies with length in a duct passing a given gas flow. To study the behaviour of the gas and particles in such a system relationships must be derived which allow for the transfer of work and heat between the two phases and which take account of mass continuity, conservation of energy, momentum changes due to impressed forces at the fluid boundaries and the properties of the gas and the particles. Other workers, who in various ways have contributed to this type of analysis, are Carrier (1958), Kliegel (1960), Bailey *et al.* (1961), Soo (1961), Kliegel & Nickerson (1962), Gilbert, Davis & Altman (1955) and Trezek & Soo (1966, p. 148). The influence of angle of attack on erosion damage involves a knowledge of the trajectories of the particles in their excursion through the nozzle. The subject of particle trajectories in nozzles is

dealt with in a separate paper by the authors. The actual erosion of materials due to attack by solid particles is the subject of a paper by Neilson & Gilchrist (1968).

2. Derivation of the relationships for gas-particle flows

Consider a duct in which a mixture of gas and solid particles is flowing. Presuming that at a given cross-section (A) in the duct the gas velocity U_g, temperature T_g and pressure p and the particle velocity U_p and temperature T_p are all known, then, if in a small axial length δx the cross-sectional area of the duct changes by δA (see figure 1), we wish to determine the new values of pressure and of gas and particle velocity and temperature after length δx. In the derivation of the relevant equations allowance is made for heat transfer between the gas and the particles and for the forces of interaction between the two phases. The following assumptions are made. (i) The flow is one-dimensional in that at a given cross-section the gas conditions are uniform and the particle conditions, though different from the gas conditions are also uniform. (ii) At the solid boundaries of the duct friction forces are zero and there is no heat transfer. (iii) The particles do not interact either with one another or with the duct boundaries. (iv) The particle temperature is uniform throughout the particle. (v) The gas is perfect and the specific heat of the particle material is constant. (vi) The effect of the volume occupied by the particles on the gas pressure is negligible. (vii) Heat exchange between the particles and the gas is by convection only.

The differentials involved are the increments, within length dx, in gas pressure, velocity and temperature, in particle velocity and temperature and in duct cross-sectional area. The increment in cross-sectional area is an independent variable and, as will be shown, the increments in particle velocity and temperature may also be regarded as independent variables. Thus in this analysis we wish to express dp, dU_g, dT_g in terms of dA, dU_p and dT_p.

Referring to figure 1, the condition for mass continuity gives

$$\rho_g U_g A = (1-\lambda)\, W \tag{1}$$

and

$$\rho'_p U_p A = \lambda W \tag{2}$$

where ρ_g is gas density, ρ'_p the mass of particles per unit volume of the flow, W the total mass flow rate of gas and particles and λ the ratio of the mass flow rate of particles to the total mass flow rate W.

From the equation of state for the gas,

$$p = \rho_g R_g T_g \tag{3}$$

where R_g is the gas constant or

$$dp = R_g(1-\lambda)\, W\left[\frac{dT_g}{AU_g} - \frac{T_g dA}{A^2 U_g} - \frac{T_g dU_g}{U_g^2 A}\right] \tag{4}$$

and

$$\frac{dp}{p} = \frac{dT_g}{T_g} - \frac{dU_g}{U_g} - \frac{dA}{A}. \tag{5}$$

Momentum considerations give

$$-dp = (1-\lambda)\frac{W\,dU_g}{gA} + \frac{\lambda W\,dU_p}{gA} \tag{6}$$

where g is the gravity constant.

For conservation of energy

$$(1-\lambda)\,W\left[JC_{pg}T_g + \frac{U_g^2}{2g}\right] + \lambda W\left[JC_sT_p + \frac{U_p^2}{2g}\right] = \text{constant}, \tag{7}$$

or

$$dT_g = -\frac{U_g\,dU_g}{C_{pg}gJ} - \frac{\lambda}{1-\lambda}\left[\frac{C_s}{C_{pg}}dT_p + \frac{U_p\,dU_p}{C_{pg}gJ}\right] \tag{8}$$

where J is Joule's equivalent, C_{pg} specific heat of gas at constant pressure and C_s specific heat of particle material.

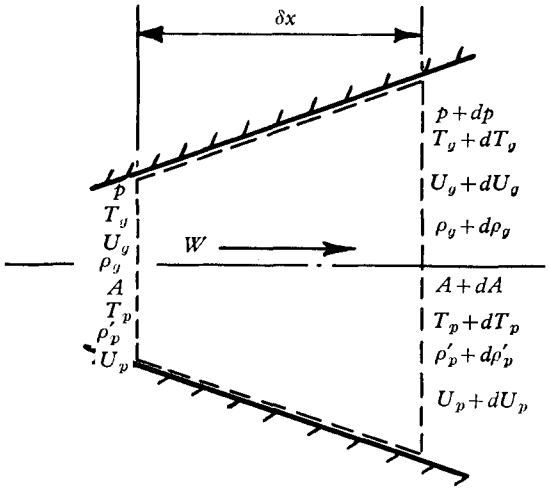

FIGURE 1. Gas and particle conditions entering and leaving a duct of elemental length.

Thus from (4) and (6), dp may be eliminated giving

$$dT_g = f(dU_g, dU_p \quad \text{and} \quad dA),$$

i.e.

$$dT_g = \frac{dA}{A}T_g - \frac{\lambda}{1-\lambda}\frac{U_g\,dU_p}{R_g g} - U_g\,dU_g\left[\frac{1}{R_g g} - \frac{T_g}{U_g^2}\right], \tag{9}$$

and from (8) and (9), dT_g may be eliminated giving

$$dU_g = f(dU_p, dT_p \quad \text{and} \quad dA),$$

i.e.

$$dU_g = \frac{gT_gR_g\dfrac{dA}{A} - \dfrac{\lambda}{1-\lambda}\left[\dfrac{-C_s}{C_{pg}}g\,R_g\,dT_p - \dfrac{U_p\,dU_p\,R_g}{JC_{pg}} + U_g\,dU_p\right]}{U_g\left[1 - \dfrac{R_g}{JC_{pg}} - \dfrac{gR_gT_g}{U_g^2}\right]}, \tag{10}$$

and for dT_g, dU_g from (10) may be substituted in (9) to give

$$dT_g = f(dU_p, dT_p \quad \text{and} \quad dA). \tag{11}$$

Finally dT_g from (11) and dU_g from (10) may be substituted in (4) to give

$$dp = f(dU_p, dT_p \quad \text{and} \quad dA). \tag{12}$$

For a numerical solution there is no need to actually make the substitutions from which (11) and (12) are derived because in such a solution dU_g may be determined first, substituted in (9) to obtain dT_g and the values of dU_g and dT_g then substituted in (4) to give dp.

In a numerical solution a small finite length δx of duct must be considered and the relationships used to determine the increments dT_g, dU_g and dp. For this type of work (10), (9) and (4) are most useful in the following forms:

$$\frac{dU_g}{dx} = \frac{\dfrac{gT_gR_g}{A}\dfrac{dA}{dx} - \dfrac{\lambda}{1-\lambda}\left[\dfrac{-C_s}{C_{pg}}gR_g\dfrac{dT_p}{dx} - \dfrac{U_pR_g}{JC_{pg}}\dfrac{dU_p}{dx} + U_g\dfrac{dU_p}{dx}\right]}{U_g\left[1 - \dfrac{R_g}{JC_{pg}} - g\dfrac{R_gT_g}{U_g^2}\right]}, \tag{13}$$

$$\frac{dT_g}{dx} = \frac{T_g}{A}\frac{dA}{dx} - \frac{\lambda}{1-\lambda}\left[\frac{U_g}{R_gg}\frac{dU_p}{dx}\right] - U_g\frac{dU_g}{dx}\left[\frac{1}{R_gg} - \frac{T_g}{U_g^2}\right] \tag{14}$$

and

$$\frac{dp}{dx} = R_g(1-\lambda)\,W\left[\frac{1}{AU_g}\frac{dT_g}{dx} - \frac{T_g}{A^2U_g}\frac{dA}{dx} - \frac{T_g}{U_g^2A}\frac{dU_g}{dx}\right]. \tag{15}$$

To study the effects of particles on the gas conditions for subsonic and supersonic gas flows, the relationships in (10) and (11) may be expressed in terms of the gas Mach number M. Equation (10) may be shown to give

$$\frac{dU_g}{U_g} = -\frac{dA}{A}\frac{1}{1-M^2} + \frac{dU_p}{U_p}\frac{U_p}{U_g}\left[\frac{\lambda}{1-\lambda}\frac{\gamma M^2 - (\gamma-1)M^2\dfrac{U_p}{U_g}}{1-M^2}\right] - \frac{C_s}{C_{pg}}\frac{T_p}{T_g}\frac{dT_p}{T_p}\left[\frac{\lambda}{1-\lambda}\frac{1}{1-M^2}\right] \tag{16}$$

and (11) reduces to

$$\frac{dT_g}{T_g} = \frac{dA}{A}\frac{(\gamma-1)M^2}{1-M^2} - \frac{U_p}{U_g}\frac{dU_p}{U_p}\left[\frac{\lambda}{1-\lambda}\frac{(\gamma-1)M^2}{1-M^2}\left\{M^2 - \gamma M^2\frac{U_p}{U_g} + \frac{U_p}{U_g}\right\}\right] - \frac{C_s}{C_{pg}}\frac{T_p}{T_g}\frac{dT_p}{T_p}\left[\frac{\lambda}{1-\lambda}\frac{1-\gamma M^2}{1-M^2}\right]. \tag{17}$$

Substitution of (16) and (17) in (5) gives

$$\frac{dp}{p} = \frac{dA}{A}\frac{\gamma M^2}{1-M^2} - \frac{U_p}{U_g}\frac{dU_p}{U_p}\left[\frac{\lambda}{1-\lambda}\frac{M^2}{1-M^2}\left\{(\gamma-1)\left(\gamma M^2 - \gamma M^2\frac{U_p}{U_g}\right) + \gamma\right\}\right] + \frac{C_s}{C_{pg}}\frac{T_p}{T_g}\frac{dT_p}{T_p}\left[\frac{\lambda}{1-\lambda}\frac{\gamma M^2}{1-M^2}\right]. \tag{18}$$

To determine the effect on the variation in Mach number:

$$M = U_g/(g\gamma R_gT_g)^{\frac{1}{2}} \tag{19}$$

or

$$\frac{dM}{M} = \frac{dU_g}{U_g} - \frac{1}{2}\frac{dT_g}{T_g}. \tag{20}$$

Thus substitution in (20) from (16) and (17) gives

$$\frac{dM}{M} = -\frac{dA}{A}\left[\frac{1+\frac{1}{2}(\gamma-1)M^2}{1-M^2}\right] + \frac{dU_p}{U_p}\frac{U_p}{U_g}\left[\frac{\lambda}{1-\lambda}\frac{M^2}{1-M^2}\left\{\gamma M^2\frac{\gamma-1}{2}\left(1-\frac{U_p}{U_g}\right)+\gamma-\left(\frac{\gamma-1}{2}\right)\frac{U_p}{U_g}\right\}\right] - \frac{C_s}{C_{pg}}\frac{T_p}{T_g}\frac{dT_p}{T_p}\left[\frac{\lambda}{1-\lambda}\frac{1+\gamma M^2}{2(1-M^2)}\right]. \quad (21)$$

Derivation of the drag equation

When a particle is introduced into a duct containing a flowing gas the motion of the particle is influenced by the drag force which interacts between the gas and the particle. This force will only be in evidence when there is relative motion between the gas and the particle.

The drag force is

$$m\frac{d^2x}{dt^2} = C_d\tfrac{1}{2}\rho_g(U_g - U_p)^2 A_p \quad (22)$$

where t is time, m the mass of a particle, A_p its cross-sectional area and C_d drag coefficient. For spherical particles the variation of C_d with the Reynolds number was obtained by Lapple & Shepherd (1940) and is shown in figure 2. The influence of Mach number on the drag coefficient has been studied by Ferri (1944) and by Charters & Thomas (1945), but for the purposes of this paper Mach number effects on drag and the effects of particle shape (other than spherical) will be ignored. The results for drag coefficients in figure 2 may be approximated to by the expression

$$C_d = f\frac{24}{Re}, \quad (23)$$

where f is given by

$$f = \frac{28Re^{-0\cdot85} + 0\cdot48}{24Re^{-1\cdot0}}, \quad (24)$$

an expression given by Gilbert *et al.* (1955).

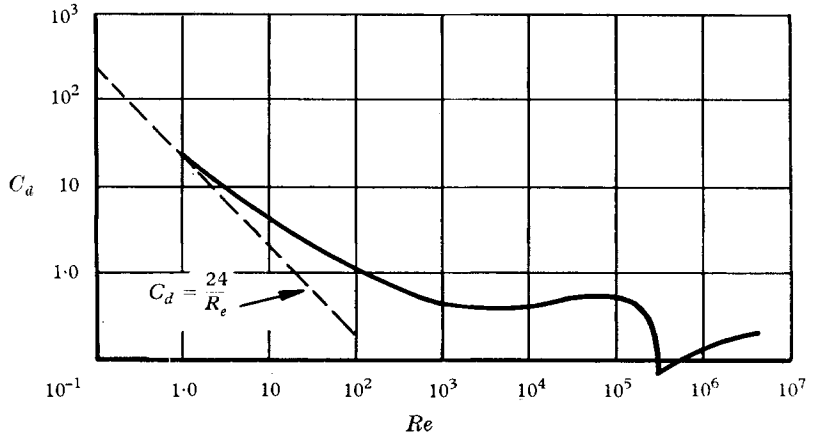

FIGURE 2. Variation of drag coefficient with Reynolds number for spheres.

Substitution of (23) in (22) gives

$$m U_p \frac{dU_p}{dx} = f\frac{24}{Re}\tfrac{1}{2}\rho_g(U_g - U_p)^2 A_p = 3\pi\mu_g d_p f(U_g - U_p), \tag{25}$$

or

$$U_p \frac{dU_p}{dx} = \alpha_m(U_g - U_p), \tag{26}$$

which is referred to as the drag equation in which

$$\alpha_m = \alpha f, \tag{27}$$

and

$$\alpha = \frac{3\pi\mu_g d_p}{m} = \frac{18\mu_g}{\rho_p d_p^2}. \tag{28}$$

Here μ_g is the coefficient of viscosity for the gas, d_p particle diameter and ρ_p particle density. Thus using (26) for a numerical solution, in which a finite length of duct, δx, is considered, the change in particle velocity may be estimated from conditions entering the section under consideration. This involves calculating α from the particle size, the particle density, the coefficient of viscosity for the gas, and obtaining f using the Reynolds number.

Derivation of the heat transfer equation

For a particle moving relative to a gas stream the heat exchanged between the gas and the particle will be mainly by convection. For spheres, in the Reynolds number range 1 to 70,000, Gebhart (1961, p. 213) and Ranz & Marshall (1952) each obtained

$$Nu = 2{\cdot}0 + 0{\cdot}6\, Re^{0{\cdot}5} Pr^{0{\cdot}333}, \tag{29}$$

where Nu is the Nusselt number and Pr the Prandtl number. This gives

$$h = \frac{K_g}{d_p}(2{\cdot}0 + 0{\cdot}6 Re^{0{\cdot}5} Pr^{0{\cdot}333}), \tag{30}$$

where h is the heat transfer coefficient, K_g the coefficient of conductivity for the gas and where the figure 2·0 applies for natural convection. Thus the heat exchanged between the gas and the particle in time dt is

$$hA_s(T_p - T_g)\,dt = mC_s(-dT_p) \tag{31}$$

where A_s is the surface area of the particle. This gives

$$U_p \frac{dT_p}{dx} = -\frac{hA_s(T_p - T_g)}{mC_s}. \tag{32}$$

Hence substituting for h from (30) into (32) gives the heat transfer equation

$$U_p \frac{dT_p}{dx} = -\frac{6K_g}{\rho_p C_s d_p^2}[(2{\cdot}0 + 0{\cdot}6 Re^{0{\cdot}5} Pr^{0{\cdot}333})(T_p - T_g)]. \tag{33}$$

Summary of the procedure of solution by numerical methods

The appropriate equations for a numerical analysis are (26), (33), (13), (14) and (15). For a cross-section in a duct at which the gas and particle conditions are known we consider the increments in the various parameters in a short length δx of the duct. From (26) and (33), dU_p/dx and dT_p/dx may be obtained and dA/dx would be known from the duct geometry. Substitution of these latter values in (13) gives dU_p/dx and using (14) and (15), dT_g/dx and dp/dx may be determined.

These slopes were assumed to apply over the small length δx enabling estimates of gas and particle conditions at $x+\delta x$ to be obtained. The transport properties of the gas may be allowed for by expressing them as functions of the gas temperature. An iterative procedure gives average values of α_m, K_g, Pr and μ_g for the interval and the process may be continued until successive sets of conditions agree to the required accuracy. The procedure is then repeated for the next interval and so on. This was the general method adopted to solve specific problems and the calculations were performed on a digital computer.

Solutions for the drag equation where it is assumed that the effects of particle on the gas conditions are negligible

Where the interchange of heat is negligible and the particle, while absorbing work from the gas, is assumed to leave the gas unaffected in any way by this interchange of energy the only relevant relationship is the drag equation for the particle. Two cases are found to be amenable to an analytical solution if the duct length is small but finite. In case (i) a parallel duct is considered in which the gas conditions remain constant and in case (ii) a duct of varying cross-section in which the acceleration of the gas is directly proportional to the length of the duct is dealt with.

Case (i). The drag equation is

$$U_p \frac{dU_p}{dx} = \alpha_m (U_g - U_p). \tag{26}$$

Let $\phi = (U_g - U_p)/U_g$, then since U_g is constant and treating α_m as a constant, (26) may be shown to give

$$x = \frac{U_g}{\alpha_m}\left[\log_e \frac{\phi_0}{\phi} - (\phi_0 - \phi)\right] \tag{34}$$

where 0 denotes initial conditions. This relationship is confined to ducts of small finite length, x, in which the parameter f, in (27), is an average value corresponding to the average Reynolds number in the duct, which in turn depends on the average value of $U_p - U_g$.

Case (ii). For a duct in which the velocity and acceleration of the gas vary linearly with duct length then

$$U_g = U_{g0} + ax \tag{35}$$

where a is the acceleration per unit length of duct. Substitution of (35) in (26) gives

$$U_p \frac{dU_p}{dx} = \alpha_m (U_{g0} + ax - U_p). \tag{36}$$

This equation is a non-homogeneous equation in U_p and x. It can be made homogeneous by obtaining a new origin of the x co-ordinate given by the expression

$$X = x + c/a, \tag{37}$$

where $c = -\alpha_m U_{g0}$. Substitution of (37) in (36) and integrating may be shown to give

$$X\left\{\left[\frac{U_p}{X}+Q\right]\left[\frac{U_p}{X}+Q'\right]\right\}^{\frac{1}{2}}\left[\frac{U_p}{X}+Q\right]^{\alpha_m/4Z^2} = X_0\left\{\left[\frac{U_{p0}}{X_0}+Q\right]\left[\frac{U_{p0}}{X_0}+Q'\right]\right\}^{\frac{1}{2}}\left[\frac{U_{p0}}{X_0}+Q\right]^{\alpha_m/4Z^2}, \tag{38}$$

where
$$Z = \alpha_m(a + \tfrac{1}{4}\alpha_m), \tag{39}$$
$$Q = \tfrac{1}{2}\alpha_m + Z^{\frac{1}{2}} \tag{40}$$
and
$$Q' = \tfrac{1}{2}\alpha_m - Z^{\frac{1}{2}}. \tag{41}$$

Again the dependence of f, equation (27), on Reynolds number restricts the solution of (38) to ducts of small finite length; but in addition to using an average value of f, average values of viscosity and density of the gas must also be used, since in this case, the pressure and temperature of the gas change as the gas velocity changes.

3. Solutions of the relationships for particular gas flow conditions and duct configurations

Duct 1. *A duct of constant cross-section*

Equations (26), (33), (13), (14), (15) and (21) were solved for a 6 in. long parallel duct for the following conditions. For the gas the entry pressure, temperature and velocity were 14·7 lbf/in.^{2}, 520 °R and 350 ft./s respectively. Spherical particles of 210 μ diameter, density 250 lb./ft.^{3}, specific heat 0·5 Btu/lb. °R were assumed to enter the duct at velocity 40 ft./s and with a temperature of 540 °R. The equations were solved for various values of the mass flow ratio λ and the results

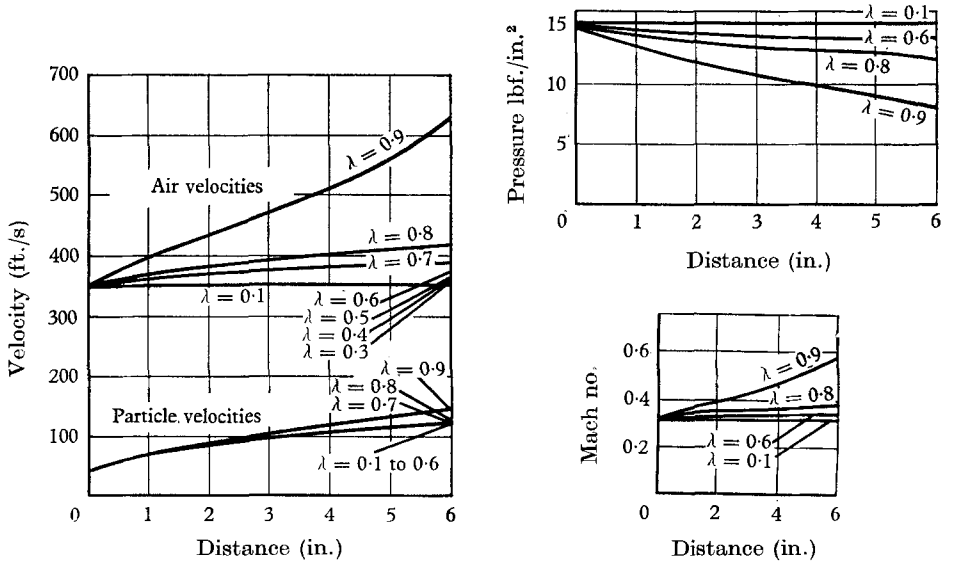

FIGURE 3. Variation of conditions in a parallel duct for various λ values. Initially subsonic flow.

are shown in figure 3. These results were for a gas flow which was initially subsonic and the computations were repeated using an initial air velocity of 1400 ft./s, an initial particle velocity of 900 ft./s for λ of 0·1. These results for initially supersonic flow are shown in figure 4.

For subsonic flow the pressure decreases and the Mach number increases with length in the duct. For supersonic flow the variations in these parameters are reversed. For subsonic flow the results show that the air velocity is appreciably affected by the value of λ especially for values of λ above 0·8. The particle velocity, on the other hand, is hardly affected by the value of λ, particularly for values less than 0·8.

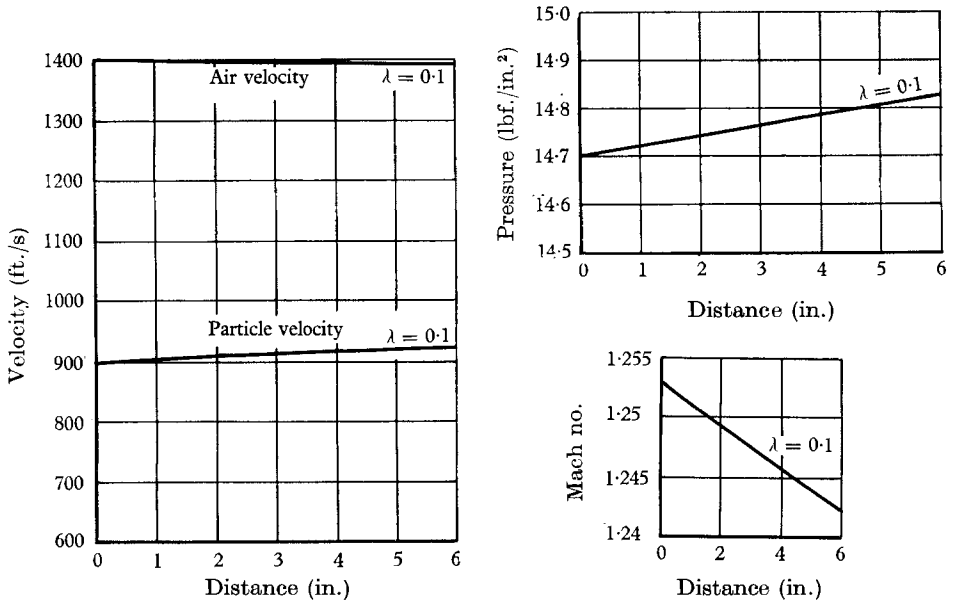

FIGURE 4. Variation of conditions in a parallel duct for $\lambda = 0{\cdot}1$. Initially supersonic flow.

For a 6 in. long parallel duct with constant air conditions, equal to the air conditions at entry to the duct for the subsonic case quoted above, the drag relationship in the form of (34) was solved for (*a*) 210 and 70 μ spheres each of density 250 lb./ft.^{3} and for initial particle velocities of 40 and 140 ft./s and for (*b*) 210 μ spheres with densities of 250 and 375 lb./ft.^{3} with initial particle velocities 40, 140 and 250 ft./s. For these cases where the gas conditions are assumed to be unaffected by the particles, the results are given in figures 5 and 6. To study the effect on particle velocity of ignoring changes in the gas condition, the results for 210 μ particles of density 250 lb./ft.^{3} and initial velocity 40 ft./s, in figures 5 and 3, may be compared. It will be seen that the particle velocity computed by either method gives substantially the same result, expecially for λ values less than 0·8. From results not quoted here, in which there was an appreciable difference between the initial gas and particle temperatures, it was shown that the temperature difference had a considerable effect on gas velocity but had little effect on particle velocity. From figures 5 and 6, initial particle velocity is seen to have a marked effect on the variation in particle velocity with length in the duct. The particle velocity is also seen to increase as the particle size reduces at a given particle density and for a given particle size, a decrease in particle density increases the velocity. The effects of particle size and density may be summarized by saying that, as the product $\rho_p d_p^2$ in (28) reduces, the particle velocity increases.

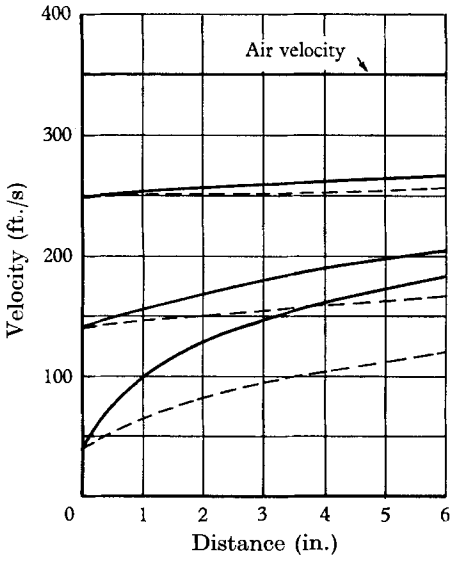

FIGURE 5

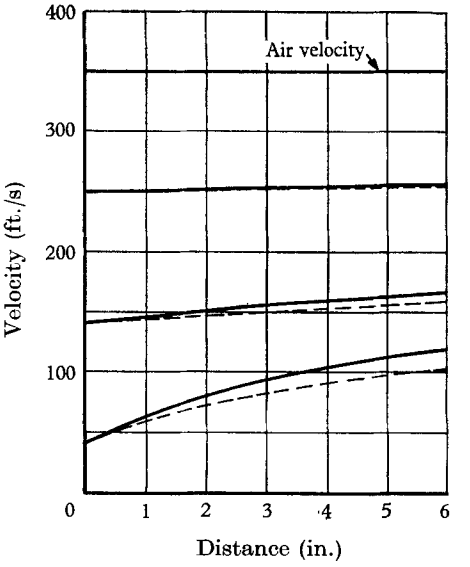

FIGURE 6

FIGURE 5. Effect of particle size on particle velocity in a constant velocity air stream. ρ_p = 250 lb./ft.^{3}; ρ_g = 0·0764 lb./ft.^{3}; μ_g = 0·00001202 lb./s. ft. ——, 70 μ sphere diameter; – – –, 210 μ sphere diameter.

FIGURE 6. Effect of particle density on particle velocity in a constant velocity air stream. Particle diameter 210 μ; ρ_g = 0·0764 lb./ft.^{3}; μ_g = 0·00001202 lb./s. ft. ——, 250 lb./ft.^{3} density; – – –, 375 lb./ft.^{3} density.

Duct 2. A convergent-divergent nozzle

The profile of the nozzle used in the computations is shown in figure 7 and the expressions for nozzle radius given in the figure allow A and dA/dx to be obtained at any value of x. The inlet cross-sectional area is finite and at this section the air

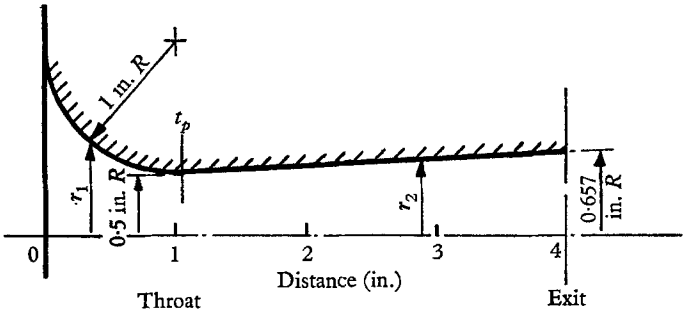

FIGURE 7. Convergent-divergent axi-symmetric nozzle (duct 2). Equations defining the above profile are: $r_1 = 1{\cdot}5 - [1-(1-x)^2]^{\frac{1}{2}}$, $0 < x < x_{tp}$; $r_2 = 0{\cdot}0529x + 0{\cdot}4449$, $x_{tp} < x < x_e$.

temperature is assumed to be 520 °R and the particle velocity and temperature 25 ft./s and 600 °R respectively. The particle size and density were taken as 210 μ and 250 lb./ft.^{3} respectively and the equations which allow for the effects

that the particles have on the air were solved for λ values of 0·1, 0·3 and 0·5. For a gas particle flow in a convergent–divergent nozzle, (21) may be used to show that at the inlet cross-section there is only one value of Mach number which will allow the flow to pass from a subsonic to a supersonic condition. This is the inlet Mach number to which flow will always adjust provided sufficient pressure drop is applied across the nozzle. This critical Mach number, which varies with λ, determines the air inlet velocity and the variation in these parameters is shown in the following table:

λ	Critical Mach no.	Air inlet velocity (ft./s)
0·1	0·1053	117·68
0·3	0·1016	113·56
0·5	0·0943	106·00

The results obtained are shown in figure 8. It will be seen that there is a considerable decrease in particle velocity with increasing values of λ. At high λ values this is apparently contrary to the result obtained in a parallel duct (figure 3) but in the case of the convergent-divergent nozzle the air velocity also suffers a considerable reduction at a given cross-section so reducing the drag on the particle. Up to values of λ of 0·3, however, there is not a great reduction in particle velocity. It will be noted that as λ increases, the point at which the gas Mach number becomes unity moves farther downstream from the geometric throat.

For comparison, the drag equation was solved for the same initial conditions assuming an isentropic variation in gas velocity within the nozzle. The particle velocity results obtained were almost identical with the $\lambda = 0{\cdot}1$ results in figure 8 (*a*), showing that for small λ values one may ignore the effects of particles on the gas when computing particle velocities.

Duct 3. *A duct in which the acceleration and velocity of the gas vary linearly with duct length*

Here the effects of particles on the gas conditions were neglected and (38) was used for the following subsonic gas conditions: initial air pressure, temperature and velocity 25 lbf./in.^{2}, 520 °R and 116·6 ft./s respectively; final pressure at the duct exit 14·7 lbf./in.^{2}; duct cross-sectional areas arranged to give a value of the constant a, in (35) and (39), of 2799 ft./s per foot length.

For particles of 210 μ diameter of density 250 lb./ft.^{3} and with initial particle velocity 46·6 ft./s [$U_{p0}/U_{g0} = 0{\cdot}4$], the variation in air and particle velocity is shown in figure 9 for a duct $3\frac{1}{2}$ in. long and in figure 10 the effect of initial particle velocity for U_{p0}/U_{g0} values ranging from 0 to 1 is shown. To illustrate the combined effect of particle density and diameter, particle velocities were obtained for the same air conditions and with $U_{p0}/U_{g0} = 0{\cdot}2$ for various values of the parameter α_m in (27) and (28). These results are shown in figure 11.

The initial rate of change of particle velocity is greatest for the greatest initial

relative velocity. At large values of duct length the variation in particle velocity is almost independent of the initial relative velocity and the particle velocity then varies linearly with duct length. For constant initial particle velocity, increasing α_m gives increasing particle velocity at any cross-section in the duct. For particles

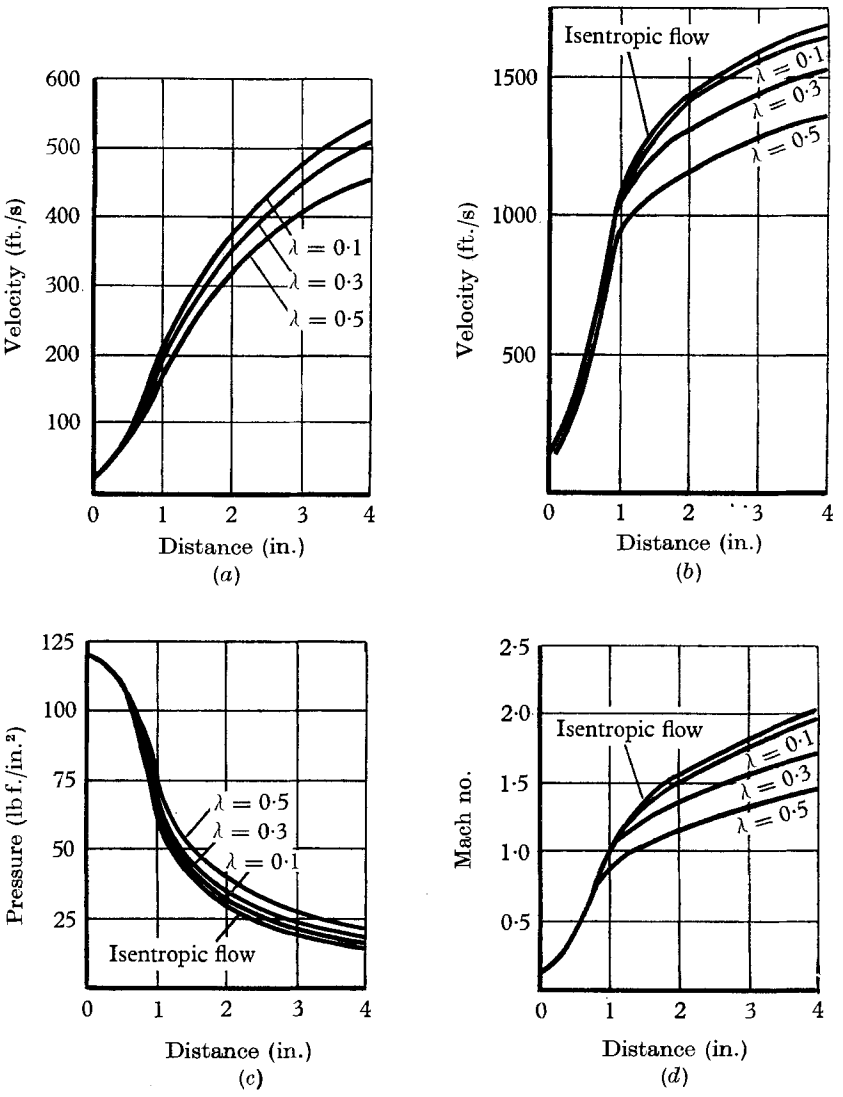

FIGURE 8. Variation of conditions through duct 2 as λ is varied. (*a*) Particle velocities. (*b*) Air velocities.

of the same density, increasing α_m corresponds to decreasing particle size, so that the smaller the particle size in the same material the greater is the acceleration suffered by the particle. For particles of the same size, increasing α_m corresponds to decreasing density and thus the lighter the particle the greater is its acceleration.

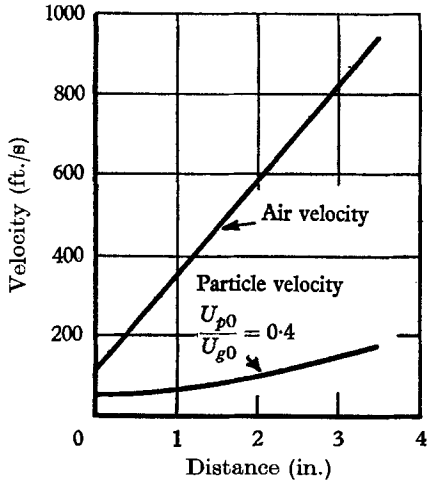

FIGURE 9

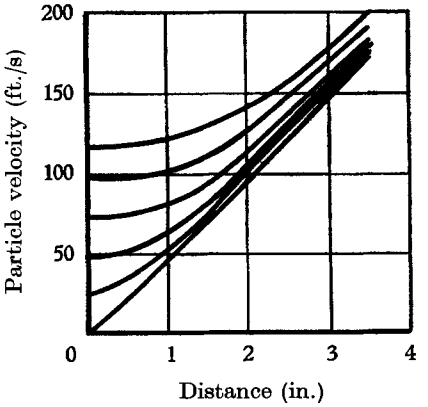

FIGURE 10

FIGURE 9. Air and particle velocity variation in a linearly accelerating air stream.

FIGURE 10. Particle velocity variations for different initial particle velocities.

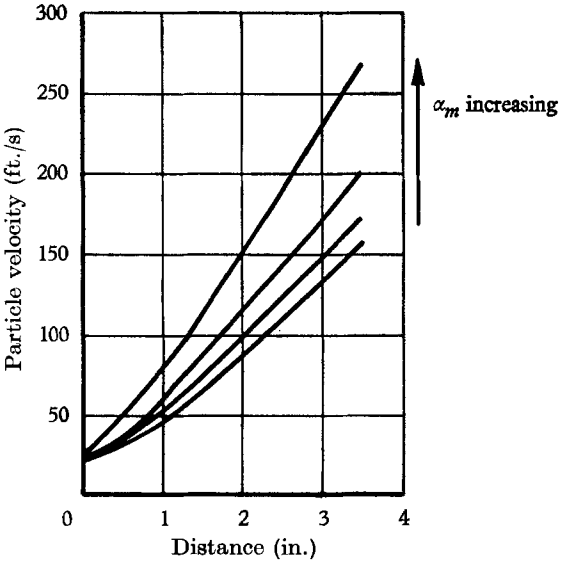

FIGURE 11. Particle velocity variations for $U_{p0}/U_{g0} = 0{\cdot}2$ showing effect of α_m ($\alpha_m = 18\mu_g f/\rho_p d_p^2$).

4. Comparison of computed particle velocities and experimentally observed values

Two-dimensional nozzles of the type quoted as duct 3 in the previous section were designed to give linear acceleration with nozzle length. The profiles of the three nozzles used are shown in figure 12. For each nozzle the inlet total head pressure and temperature were 25 lbf./in.^{2} and 520 °R respectively and the exit

pressure was 14·7 lbf./in.^{2}. Under these conditions, if one assumes isentropic flow in the nozzle, the exit air velocity is determined and for a linear variation in velocity the duct length chosen for a particular nozzle then determines the value of the constant a in (35) and (39). The three nozzles, which are referred to as ducts A, B and C, had lengths of 4, 5 and 6 in. respectively. The corresponding values of a are shown in figure 12 and the air velocity variations are shown in figure 13. A sketch of the actual experimental rig is shown in figure 14.

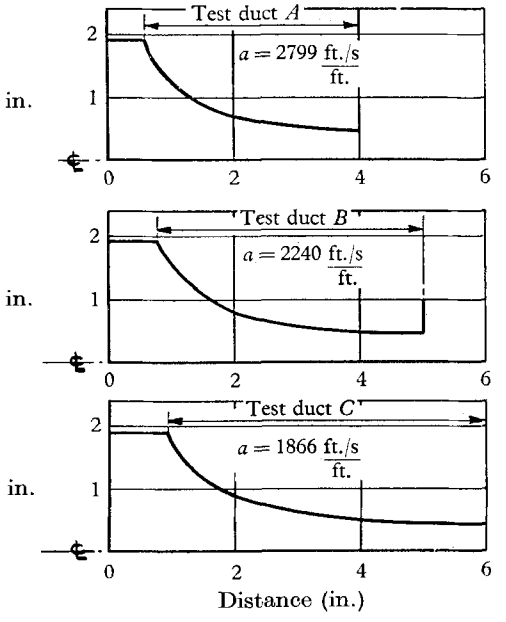

FIGURE 12

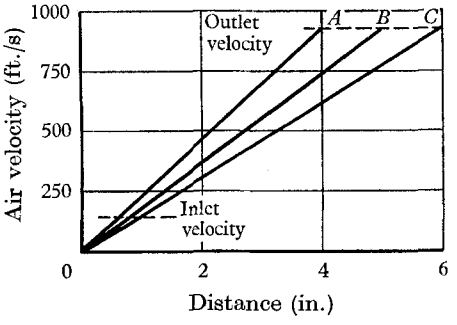

FIGURE 13

FIGURE 12. Ducts giving linear acceleration of the air.

FIGURE 13. Air velocity variations in ducts A, B and C.

In the experiments the mass flow rate of particles was kept to low values and the actual velocities of particles at the nozzle exit were obtained using a double exposure photographic technique in which two exposures of a particle were recorded on one negative with a known time interval between exposures. Theoretical particle exit velocities were computed using (38). Here a difficulty arose about the value of the particle velocity entering the nozzle. This was resolved by computing exit particle velocities for each case for (*a*) a low assumed value of initial particle velocity and for (*b*) a high value of particle velocity where the particle velocity was only slightly less than the inlet air velocity.

The first tests were performed using spherical iron shot of mean diameter 500 μ, density 677 lb./ft.^{3} and using assumed values of initial particle velocity of 20 and 130 ft./s. These experiments were performed using ducts A and B only (figure 12) and the results are given in figure 15. The initial particle velocities are seen to have a marked influence on the theoretical outlet velocities and the experimental results lie within the range of particle velocities predicted for each duct.

The theoretical results computed previously had shown that the predicted outlet particle velocities for small light particles were relatively independent of initial particle velocity. For this reason glass spheres of 195 μ diameter and of

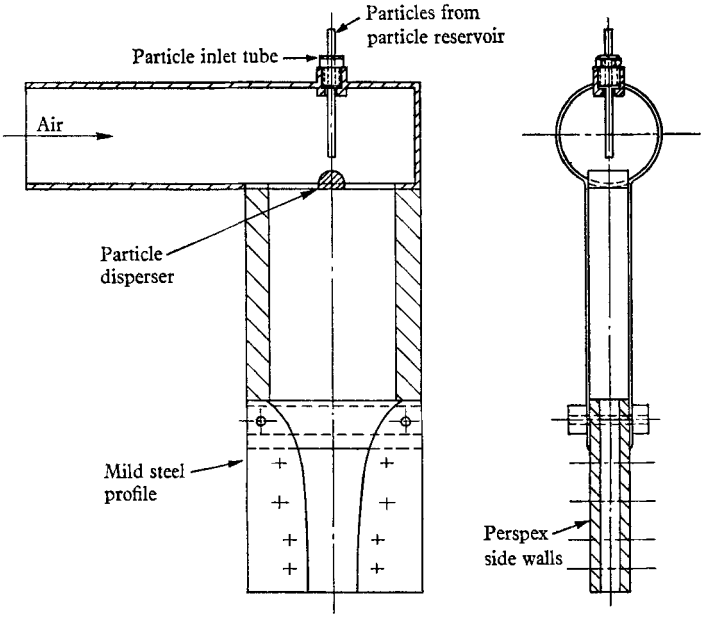

FIGURE 14. Test rig for use with linear acceleration ducts.

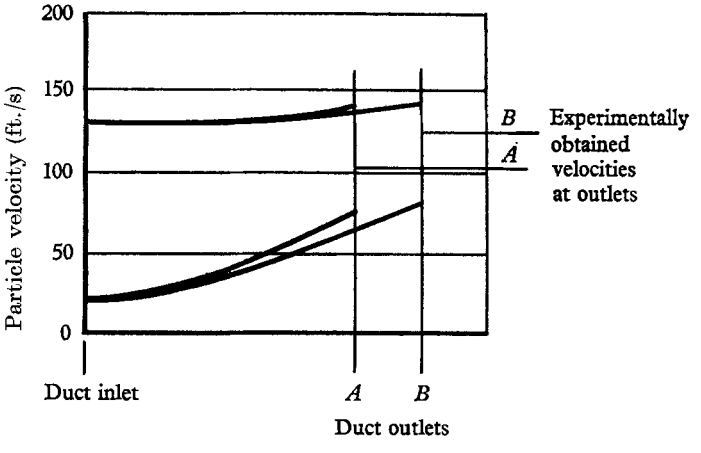

FIGURE 15. Velocities of 500 μ spherical chilled iron shot for two different flows.

density 187·5 ft.^{3}/lb. were examined in ducts A, B and C, and the results are shown in figure 16. The actual exit velocities of the spheres for the three ducts are seen to lie very close to, or within, the theoretical outlet velocity ranges predicted using the two extreme values of initial particle velocity.

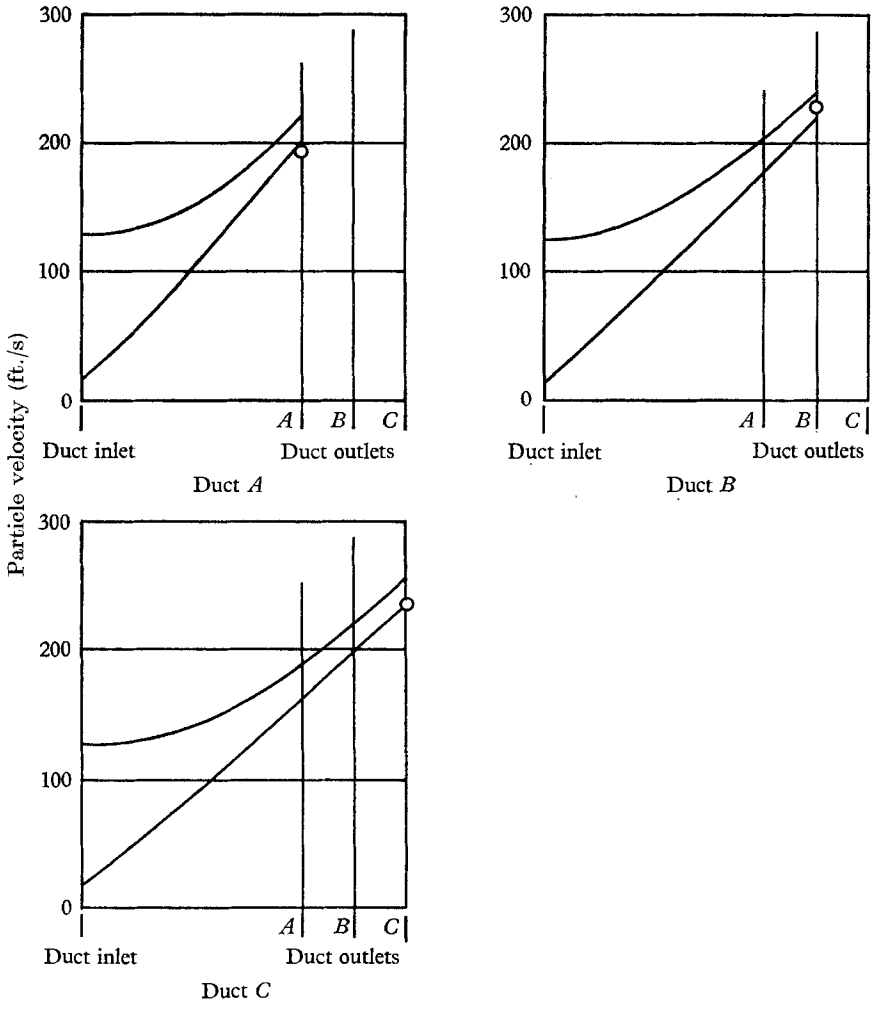

FIGURE 16. Velocities of 195 μ glass spheres for three different flows. ○, experimentally obtained particle velocities at duct outlets.

5. Concluding remarks

For subsonic flow of a gas in a duct of constant cross-section, heating the gas causes the gas velocity and Mach number to increase with length through the duct. The heating effect may be obtained in a number of ways. The gas may be heated directly through the walls of the duct while eddies or turbulence, if significant, cause a degeneration of kinetic energy into frictional heat which, for one-dimensional flow, must always be regarded as an effect at the duct walls, usually accounted for by a wall shear stress expressed in terms of a friction factor for the flow. When particles are introduced into the gas stream two further heating effects are present. There is the direct transfer of heat from the particles to the gas. In addition, however, the drag interaction between the gas and the particles is akin to the frictional effect of eddies and turbulence in single-phase flow.

For gas particle flows all of these heating effects can be in evidence simultaneously.

In the examples chosen in this paper the duct lengths were relatively small so that the effects of external heating and of frictional heating in the gas phase were neglected. Under these circumstances it has been shown that the gas velocity is appreciably affected if the ratio of particle mass flow to total mass flow (λ) is greater than 0·8. For values of λ less than 0·8, however, the particle velocity varies very little from that which would be attained if there had been no change in the gas velocity. Where the proportion of particles is large the heating effect on the gas is such that the gas velocity and Mach number increase rapidly with length through the duct and there is a corresponding decrease in gas pressure. These effects are illustrated clearly by the constant area duct results shown in figure 3 for a λ value of 0·9. Here the proportion of particles is high and the flow may rapidly attain a choking condition akin to that in single-phase fanno flow. Hence for large λ values it is not possible to disregard the effects of the particles on the gas velocity in determining the final particle velocity. Even under these circumstances, however, it will be noted from figure 3 that the rate of increase of particle velocity with duct length, (dU_p/dx), is much smaller than the corresponding gas velocity gradient, (dU_g/dx), which becomes very large towards the end of the duct. This means in turn that the relative velocity, $(U_g - U_p)$, tends to increase towards the end of the duct. This phenomenon is also apparent in the results obtained for linearly accelerating gas flows to which small segments of a constant area duct with high particle flow rates will approximate. Thus from figure 9 we see that, for a given particle, the relative velocity or lag increases with duct length and in figure 10 the results indicate that, while the initial relative velocity markedly affects the particle velocity distribution in the inlet section of the duct, the final relative velocity will be independent of initial relative velocity if the duct is long enough. Figure 11 shows, however, that the final relative velocity is dependent on the type of particle so that a small light particle will have a smaller final relative velocity than a large heavy particle.

Trezek & Soo (1966) have investigated gas-particle flows in a long duct of constant cross-section (duct diameter 0·75 in. and duct length 20 ft.). Their experiments were so arranged that choking conditions were always attained at the exit of the duct. With such a duct internal friction in the gas phase must be of importance and they account for this by including a friction term $(2fLU_g^2/D)$ in the momentum equation. If the local friction factor, f, is dependent only on the local gas conditions (so that at a given point in the duct, f is influenced by the presence of particles only in so much as the particles have caused the gas conditions to change) then using the usual relationship between f and Reynold's number the appropriate equations for the flow, given in this paper as equations (26), (33), (13), (14) and (15), may be solved numerically. However, the results obtained by Trezek & Soo suggest that the particles scrub the walls of the duct so that an additional frictional effect has to be taken into account. This local frictional effect of particles scrubbing the walls of the duct should be dependent on the local particle velocity. Trezek & Soo, however, allow for the combined effects of gas and particle wall friction by assuming that a modified form of f in the

relationship $2fLU_g^2/D$ can be used. Since the variation of this modified friction factor f with Reynold's number is unknown, they proceed to solve the flow equations using the observed values of pressure distribution in the pipe. They are then able to confirm that the local friction factors differ from the usual ones, which in turn implies that the particles do have a scrubbing action on the walls. One of the most interesting observations made by Trezek & Soo, was the appreciable lag between the phases at the end of the duct. This confirms the statements made above about the behaviour of the particle velocity in regions where the gas velocity gradient is high.

For initially supersonic flow in a duct of constant cross-section the pressure increases and the gas velocity and Mach number decrease. In a convergent-divergent nozzle, the effect of entrained particles is to increase the pressure and decrease the gas velocity and Mach number at all sections in the nozzle compared with the values of these parameters which would pertain for isentropic flow in the nozzle. The reduction in gas velocity increases as the proportion of particles in the flow increases but the effect on particle velocity may be neglected for mass flow ratios less than 0·3.

The results show that for any duct with a moderate flow rate of particles any reasonable estimate of the gas velocity distribution is sufficient to determine the particle velocity distribution.

This work was performed at the University of Strathclyde under the general direction of Professor A. S. T. Thomson of the Mechanical Engineering Department. The work was initiated by the Ministry of Aviation and Imperial Metal Industries (Kynoch) Ltd., Summerfield Research Station, England.

REFERENCES

Bailey, W. S., Wilson, E. N., Serra, R. A. & Zuprik, T. F. 1961 Gas particle flow in an axi-symmetric nozzle. *J. Am. Rocket Soc.* **31**, 793.

Carrier, G. F. 1958 Shock waves in dusty gases. *J. Fluid Mech.* **4**, 376.

Charters, A. C. & Thomas, R. N. 1945 The aerodynamic performance of small spheres from subsonic to high supersonic velocities. *J. Aero. Sci.* **12**(4), 468.

Ferri, A. 1944 The influence of the Reynold's number at high Mach numbers. *J. R. Aero. Soc.* **48**, 45.

Gebhart, B. 1961 *Heat Transfer*. New York: McGraw Hill.

Gilbert, M., Davis, L. & Altman, D. 1955 Velocity lag of particles in linearly accelerated combustion gases. *Jet Propulsion*, **25**, 26.

Kliegel, J. R. 1960 One-dimensional flow of a gas-particle system. *Inst. Aero. Sci. Paper*, no. 60–5.

Kliegel, J. R. & Nickerson, G. R. 1962 Flow of gas-particle mixtures in axially-symmetric nozzles. *Progress in Astronautics and Rocketry*, Vol. 6. New York: Academic Press.

Lapple, C. E. & Shepherd, C. B. 1940 Calculation of particle trajectories. *Ind. & Eng. Chem.* **32** (5), 605.

Neilson, J. H. & Gilchrist, A. 1968 An analytical and experimental investigation of the trajectories of particles entrained by the gas flow in nozzles. Awaiting publication.

Neilson, J. H. & Gilchrist, A. 1968 Erosion by a stream of solid particles. *Wear*, **11** (2), 111.

RANZ, W. E. & MARSHALL, W. R. 1952 Evaporation from drops. *Chem. Eng. Progress*, **48**, 141.

SOO, S. L. 1961 Gas dynamic processes involving suspended solids. *J. Am. Inst. Chem. Eng.* **7** (3), 384.

TREZEK, G. J. & SOO, S. L. 1966 Gas dynamics of accelerating particulate flow in circular ducts. *Proc. Heat Transfer and Fluid Mechanics Institute*, Stanford University Press.